4-2010

The Ontogeny of Muscle Structure and Locomotory Function in the Long-Finned Squid Doryteuthis Pealeii

J. T. Thompson

I. K. Bartol
Old Dominion University, ibartol@odu.edu

A. E. Baksi

P. S. Krueger

Original Publication Citation

Thompson, J. T., Bartol, I. K., Baksi, A. E., Li, K. Y., & Krueger, P. S. (2010). The ontogeny of muscle structure and locomotory function in the long-finned squid *Doryteuthis pealeii*. *Journal of Experimental Biology, 213*(7), 1079-1091. doi:10.1242/jeb.034553

The Journal of Experimental Biology 213, 1079-1091

doi:10.1242/jeb.034553

The ontogeny of muscle structure and locomotory function in the long-finned squid *Doryteuthis pealeii*

J. T. Thompson[1,*], I. K. Bartol[2], A. E. Baksi[1], K. Y. Li[1] and P. S. Krueger[3]

[1]Department of Biology, Franklin & Marshall College, PO Box 3003, Lancaster, PA 17604-3003, USA, [2]Department of Biological Sciences, Old Dominion University, Norfolk, VA 23529, USA and [3]Department of Mechanical Engineering, Southern Methodist University, Dallas, TX 75275, USA

*Author for correspondence (joseph.thompson@fandm.edu)

Accepted 11 December 2009

SUMMARY

Understanding the extent to which changes in muscle form and function underlie ontogenetic changes in locomotory behaviors and performance is important in understanding the evolution of musculoskeletal systems and also the ecology of different life stages. We explored ontogenetic changes in the structure, myosin heavy chain (MHC) expression and contractile properties of the circular muscles that provide power for jet locomotion in the long-finned squid *Doryteuthis pealeii*. The circular muscle fibers of newly hatched paralarvae had different sizes, shapes, thick filament lengths, thin:thick filament ratio, myofilament organization and sarcoplasmic reticulum (SR) distribution than those of adults. Viewed in cross section, most circular muscle cells were roughly triangular or ovoid in shape with a core of mitochondria; however, numerous muscle cells with crescent or other unusual cross-sectional shapes and muscle cells with unequal distributions of mitochondria were present in the paralarvae. The frequency of these muscle cells relative to 'normal' circular muscle cells ranged from 1:6 to 1:10 among the 19 paralarvae we surveyed. The thick filaments of the two types of circular fibers, superficial mitochondria-rich (SMR) and central mitochondria-poor (CMP), differed slightly in length among paralarvae with thick filament lengths of 0.83±0.15 μm and 0.71±0.1 μm for the SMR and CMP fibers, respectively (P 0.05; ANOVA). During ontogeny the thick filament lengths of both the CMP and SMR fibers increased significantly to 1.78±0.27 μm and 3.12±0.56 μm, respectively, in adults (P<0.0001 for both comparisons; ANOVA with Tukey's highly significant difference *post hoc* tests). When sectioned parallel to their long axes, the SMR and CMP fibers of both paralarvae and adults exhibited the myofilament arrangements typical of obliquely striated muscle cells but the angle of obliquity of the dense bodies was 22.8±2.4 deg. and 4.6±0.87 deg. for paralarvae and adults, respectively. There were also differences in the distribution of the anastomosing network of SR. In paralarvae, the outer and central zones of SR were well developed but the intramyoplasmic zone was greatly reduced in some cells or was scattered non-uniformly across the myoplasm. Whereas in adults the intramyoplasmic SR region was composed primarily of flattened tubules, it was composed primarily of rounded vesicles or tubules when present in the paralarvae. The ontogenetic differences in circular muscle structure were correlated with significant differences in their contractile properties. In brief tetanus at 20°C, the mean unloaded shortening velocity of the paralarval circular muscle preparations was 9.1 L_0 s^{-1} (where L_0 was the preparation length that generated the peak isometric stress), nearly twice that measured in other studies for the CMP fibers of adults. The mean peak isometric stress was 119±15 mN mm^{-2} physiological cross section, nearly half that measured for the CMP fibers of adults. Reverse transcriptase-polymerase chain reaction analysis of paralarval and adult mantle samples revealed very similar expression patterns of the two known isoforms of squid MHC. The ontogenetic differences in the structure and physiology of the circular muscles may result in more rapid mantle movements during locomotion. This prediction is consistent with jet pulse durations observed in other studies, with shorter jet pulses providing hydrodynamic advantages for paralarvae.

Key words: cephalopod, jet locomotion, mechanics, obliquely striated muscle, hydrodynamics, ontogeny, muscle ultrastructure.

INTRODUCTION

Muscle fibers can be modified to produce a broad continuum of contractile properties. These modifications, in conjunction with changes in other parts of the motor system, have resulted in muscles that can generate force economically (Twarog, 1967), produce relatively high force over an impressive range of lengths (Hoyle et al., 1965; Lanzavecchia, 1977; Herrel et al., 2002; Woods et al., 2008), shorten with great speed (Rome et al., 1996; Schaeffer et al., 1996; Elemans et al., 2004), act as powerful motors (Lutz and Rome, 1994; Marsh and Olson, 1994), as brakes or shock absorbers (Full et al., 1998), as struts (Roberts et al., 1997; Biewener et al., 1998) or as springs (Tu and Dickinson, 1994). A recognized, but understudied, phenomenon is that muscle fibers can be modified extensively during ontogeny (e.g. Greer-Walker, 1970; Goldspink and Ward, 1979; Anapol and Herring, 1989; Gilly et al., 1991; Kier, 1996; Thompson and Kier, 2006; Etnier et al., 2008). The ultimate causes of ontogenetic muscle modifications are not always apparent from a functional or ecological perspective but they may represent developmental constraints, selection for different levels of performance during ontogeny or both. Understanding the extent to which changes in muscle form and function underlie ontogenetic changes in locomotory behaviors and performance is important to understanding the evolution of musculoskeletal systems and also the ecology of different life stages.

We explored the ontogeny of muscle structure, the expression of isoforms of myosin heavy chain (MHC) and the function of the

mantle in squid, with respect to how changes in these parameters affect jetting behavior and performance. Unlike vertebrates and some arthropods, in which striated muscle fibers may be altered during ontogeny *via* expression of different isoforms of MHC (Bárány, 1967; Goldspink, 1968; Goldspink, 1983; Gauthier et al., 1978; Bandman, 1985; Gondret et al., 1996), changes in the ratio of the alkali light chains (Sweeney et al., 1988) or changes in calcium sensitivity *via* expression of isoforms of troponinT (Fitzhugh and Marden, 1997), squids appear to modify muscle mechanical properties by altering the lengths of the thick filaments. For example, the thick filaments of the obliquely striated transverse muscles of the arms of the oval squid *Sepioteuthis lessoniana* increase in length during ontogeny, from 2.2 μm in hatchlings to 6.4 μm in adults, while the thick filament lengths of the cross-striated transverse muscles of the tentacles decrease from 2.4 μm to 1.2 μm during the same interval (Kier, 1996). The ontogenetic change in thick filament length of the tentacle muscle is clearly related to changing function (see Kier, 1982) of the tentacles but the functional basis for the arm muscle change is less clear (Kier, 1996).

Ontogeny of circular muscle structure and function

Production of jet thrust in squids requires the integration of internal (i.e. the components of the motor system, including connective tissues) and external (i.e. jet dynamics) factors. In jetting, contraction of the circular muscles of the mantle pressurizes the mantle cavity and drives water out of the mantle cavity *via* the funnel (Young, 1938). Mantle contraction rate, the amplitude of mantle cavity pressure, the mass flux of the jet (i.e. the mass of water ejected from the funnel per unit time) and jet velocity are determined largely by the contractile properties of the circular muscles of the mantle, although the muscles of the funnel can adjust the aperture and, therefore, also affect jet velocity. Thus, the contractile properties of the circular muscles directly affect the hydrodynamics of the jet wake, jet thrust and jet propulsive efficiency. Both the rate of mantle contraction and the mass flux of the escape jet, however, change in some squid during growth (Thompson and Kier, 2001a; Thompson and Kier, 2002), and evidence suggests that the contractile properties of the circular muscles may change during ontogeny (Thompson and Kier, 2006).

Two important changes in the circular muscles of the mantle occur during the ontogeny of squids. The first is the relative abundance of the two types of circular muscle fibers. Many squid species possess two types of circular muscle cells: centrally located, mitochondria-poor (CMP) fibers and superficially located, mitochondria-rich (SMR) fibers (Bone et al., 1981; Mommsen et al., 1981) [terminology from Preuss et al. (Preuss et al., 1997)]. Both fiber types are obliquely striated, have a core of mitochondria, a single nucleus and are electrically coupled to adjacent circular muscle fibers, presumably by gap junctions (Marceau, 1905; Young, 1938; Hanson and Lowy, 1957; Kawaguti and Ikemoto, 1957; Millman, 1967; Ward and Wainwright, 1972; Moon and Hulbert, 1975; Bone et al., 1995; Milligan et al., 1997). The SMR circular muscle fibers are hypothesized to provide power for ventilation of the mantle cavity and prolonged, slow-speed jetting (Bone et al., 1981; Mommsen et al., 1981; Bartol, 2001). Conversely, the CMP circular muscle fibers are hypothesized to provide power for high velocity jets, including escape jets (Bone et al., 1981; Mommsen et al., 1981; Gosline et al., 1983; Bartol, 2001). The ratio of SMR:CMP fibers decreases from about 1:1 to 1:10 in the mantle of *S. lessoniana* and *Doryteuthis* (formerly *Loligo*) *opalescens* during growth from a tiny paralarva to a large adult (Preuss et al., 1997; Thompson and Kier, 2001b). The second important change is that the thick filaments of both the SMR and CMP circular muscles increase 1.5-fold in length, at least during the ontogeny of *S. lessoniana* (Thompson and Kier, 2006).

The ontogenetic increase in thick filament length may affect the contractile properties of the circular muscles. The shortening velocity of striated muscles depends on the lengths of the thick filaments and sarcomeres, the load on the muscle and the rate of cross-bridge cycling (e.g. Josephson, 1975). Thick filament length is inversely proportional to unloaded shortening velocity and is directly proportional to peak isometric force (e.g. Josephson, 1975). Assuming all else about the fibers is equal, we hypothesize that the circular muscles of paralarval squids produce lower peak isometric stresses and higher unloaded shortening velocities than the circular muscles of adult squids. To better understand how the structure and function of the circular muscles that provide power for jet locomotion change throughout ontogeny in squids, we examined (1) muscle properties using mechanical tests, (2) muscle morphometrics using histological techniques, and (3) the expression of isoforms of MHC using reverse transcription-polymerase chain reaction in paralarvae and, wherever data were lacking from previous studies, adult life stages of the long-finned squid *Doryteuthis pealeii*.

MATERIALS AND METHODS

Animals

We performed our experiments on the paralarvae and sexually mature adults of the long-finned squid *Doryteuthis* (formerly *Loligo*) *pealeii* Leseuer. Egg fingers were collected from the waters near Woods Hole, MA, and Walpole, ME (USA) between 1 June and 30 September 2006 and 2007. They were housed in a flow-through seawater system with temperature and salinity ranging from 14 to 18°C and 28 to 32 p.p.t. (parts per thousand), respectively. Copepods, small mysid shrimp and larval brine shrimp were available as prey but feeding by the paralarvae was observed only rarely. Healthy paralarvae (i.e. squid that had normal coloration, that did not rest on the bottom of the tank and that were able to hold their vertical position in the water column *via* vigorous jetting) were used in experiments within 12 h of hatching. The mean ± s.d. dorsal mantle length (DML) of the paralarvae was 1.6±0.1 mm.

We caught male and female *D. pealeii* at night from lighted piers in South Bristol and Walpole, ME, USA, in July 2007. We trapped all of the squid with a 4.2 m-diameter cast net and then transported them immediately to the lab in 24 l buckets. Squid were housed in a 1 m × 2 m × 0.5 m tank provided with flow-through seawater at 14–18°C and 28–32 p.p.t. salinity. The animals were fed small fish (*Clupea* spp.) daily and were used within four days of capture. We used only squid that were healthy, had no visible damage to the skin or mantle and swam vigorously. The adults ranged in size from 150 to 167 mm DML.

Muscle mechanical testing

Paralarvae were anesthetized in cold seawater (3°C) (O'Dor and Shadwick, 1989; Bower et al., 1999), transferred to a drop of ice-cold modified squid saline solution containing (in mmol l^{-1}): NaCl (450), $MgCl_2 \cdot 6H_2O$ (10), Hepes (10), EGTA (10), pH adjusted to 7.8 with 2 mol l^{-1} NaOH (Milligan et al., 1997), and then killed by impaling the brain with a straight pin. The posterior tip (i.e. about 0.5 mm) of the mantle was sliced off. The mantle was then separated from the rest of the body, slit along the dorsal side and unrolled to form an approximately rectangular piece of tissue from what was once a hollow cylinder. The pen was removed and then each slit edge of the mantle was glued with Vetbond (3M, St Paul, MN, USA)

to a T-shaped foil clip (Milligan et al., 1997). The clips were attached so that the long axes of the circular muscle fibers were parallel to the long axis of the preparation. The preparation was then transferred to a temperature-controlled bath. The bath was filled with standard squid saline containing (in mmol l^{-1}): NaCl (470), KCl (10), $CaCl_2$ (10), $MgCl_2 \cdot 6H_2O$ (50), glucose (20), Hepes (10), pH adjusted to 7.8 with 2 mol l^{-1} NaOH (Milligan et al., 1997).

The muscle preparations were attached at one end to an ASI 400A force transducer (Aurora Scientific Inc., Aurora, ON, Canada) and at the other end to an ASI 322 high-speed length controller (Aurora Scientific Inc.). The length–force relationship of each tissue preparation was determined using supramaximal brief tetanic (2 ms pulses, 50 Hz, 200 ms) and twitch stimulations. Stimuli were provided *via* platinum foil electrodes that spanned the entire length and width of the preparation. The maximum unloaded shortening velocity (V_{max}) was determined at $0.9L_0$ (where L_0 was the length of the preparation at which isometric tension was highest) using slack tests (Edman, 1979). We chose $0.9L_0$ because passive tension was close to zero for all preparations at this length. We performed regular isometric control stimulations to monitor the health of the preparation. If the force produced during isometric contraction at L_0 decreased by more than 10%, we terminated the experiment and discarded all data collected subsequent to the previous control stimulation. We analyzed data from the muscle preparations of 19 paralarvae.

The muscles of the mantle are arranged primarily in two orientations: circumferentially (the circular muscles) and radially (the radial muscles) (Marceau, 1905; Williams, 1909; Young, 1938). Contraction of the circular muscles drives water out of the mantle cavity *via* the funnel while contraction of the radial muscles helps to refill the mantle cavity with water at the end of the power stroke (Young, 1938). As mentioned earlier, two types of circular muscle have been identified in loliginid and ommastrephid squids: CMP and SMR fibers (Bone et al., 1981; Mommsen et al., 1981) [terminology from Preuss et al. (Preuss et al., 1997)]. As in a previous study of the contractile properties of the CMP and SMR circular muscle fibers of adult *D. pealeii* (Thompson et al., 2008), we attempted to use a vibratome to cut sheets of circular muscles from the mantles of paralarvae. The paralarval mantles were thin (about 0.06 mm thick) and were much less stiff than the adult mantles, perhaps because they have significantly fewer intramuscular connective tissue fibers than the adults (see Thompson and Kier, 2001b). The result was that the vibratome blade tended to deform the paralarval mantles rather than slice them, and we had no success in isolating the SMR or CMP circular muscle fibers. The paralarval mantle preparations, therefore, contained intact SMR and CMP circular muscle fibers as well as radial fibers. We discuss the limitations of the paralarval intact preparations in the Discussion.

Morphometrics

Following the mechanical tests, each preparation was pinned at L_0 in a Sylgard dish. Most of the preparations were fixed for 6–8 h (3% glutaraldehyde, 0.065 mol l^{-1} phosphate buffer, 0.5% tannic acid and 6% sucrose) and then postfixed for 45 min at 4°C in a 1:1 solution of 2% osmium tetroxide and 2% potassium ferrocyanide in 0.13 mol l^{-1} cacodylate buffer (Kier, 1985). The tissue was rinsed in chilled 0.13 mol l^{-1} cacodylate buffer for 15 min, dehydrated in a graded series of acetones and embedded in epoxy resin (Embed 812, Electron Microscopy Sciences, Hatboro, PA, USA). A few of the preparations were fixed in a modified Karnovsky fixative (2% paraformaldehye, 3% glutaraldehyde, 0.065 mol l^{-1} phosphate buffer and 2% sucrose), rinsed in phosphate buffer, dehydrated in ethanol and then stained in 1% phosphotungstic acid in absolute ethanol prior to embedding in LR White (Electron Microscopy Sciences, Hatfield, PA, USA). As is typical in squid muscle, dense bodies did not stain well in the 3% glutaraldehyde fixative (Kawaguti and Ikemoto, 1957; Ward and Wainwright, 1972; Moon and Hulbert, 1975; Bone et al., 1981; Kier, 1985) but the preservation of the myofilaments, sarcoplasmic reticulum (SR), plasma membrane and mitochondria was excellent. The tissues fixed in the modified Karnovsky and stained in phosphotungstic acid showed excellent preservation and staining of the dense bodies and thick filaments but the preservation and staining of the mitochondria, plasma membrane and SR were poor. For all tissues, transverse sections of the preparations were cut, stained and examined with brightfield and electron microscopy to measure the physiological cross section (pcs) of the circular muscle fibers (for details, see Thompson et al., 2008) and to explore the ultrastructure of the cells.

We prepared the mantle tissue of three adult *D. pealeii* for histology in order to examine circular muscle cell size, shape and structure in detail, and also to confirm the thick filament lengths reported by Thompson et al. (Thompson et al., 2008). We anesthetized the animals in a 1:1 solution of 7.5%$MgCl_2 \cdot 6H_2O$:seawater (Messenger et al., 1985), decapitated them and then removed small blocks of mantle tissue from the ventral midline approximately $\frac{1}{2}$ DML from the anterior edge of the mantle. The tissue blocks spanned the thickness of the mantle wall (i.e. they included radial muscle fibers plus both types of circular fibers). They were fixed, post-fixed and then embedded in epoxy resin as described above.

The protocol we followed for measuring thick filament lengths is described in detail elsewhere (Thompson and Kier, 2006; Thompson et al., 2008). Briefly, embedded tissue blocks were sectioned in a plane perpendicular to the longitudinal axis of the mantle (i.e. parallel to the long axes of the circular muscles) using a diamond knife. Thick sections (0.5–1 μm) were cut initially and stained in an aqueous solution of 0.1% Methylene Blue and 0.1% Azure II. Sections were then examined using brightfield microscopy to determine if the long axes of the circular muscle fibers were parallel to the knife edge. Once alignment was achieved, thin sections (silver interference color) were cut, mounted on grids and stained with 2% aqueous uranyl acetate (Bozzola and Russell, 1992) and 0.4% lead citrate (Venable and Coggeshall, 1965). Thin sections were examined with either a Zeiss EM-902 (Oberkochen, Baden-Wurttemberg, Germany) or JEOL JEM-100SX (Tokyo, Japan) transmission electron microscope and photographed.

The electron micrograph negatives were scanned at 4800 dpi (dots per inch), and thick filament lengths measured using ImageJ software (Abramoff et al., 2004). We measured thick filaments from at least five CMP and SMR muscle fibers per preparation, and a total of about 1200 thick filaments from paralarvae and 700 from the three adults. The mean thick filament length per animal was used for the statistical comparisons. Although great care was taken to align the long axes of the circular muscle fibers with the section plane, the thick filament lengths we report here may nevertheless be slight underestimates.

RNA purification and RT-PCR

We used reverse transcription-polymerase chain reaction (RT-PCR) to determine if different isoforms of MHC are expressed in the mantle during ontogeny. We anesthetized two adult *D. pealeii* (155 and 167 mm DML) in cold water, decapitated them, quickly excised small blocks of tissue and then placed the blocks into RNAlater™ (Ambion, Inc., Austin, TX, USA). The tissues included the central

zone of the mantle (containing CMP and radial muscle fibers but no SMR fibers), portions of the mantle containing all muscle fiber types and the funnel retractor muscle. We also placed 25 whole paralarval mantles (including the fins, skin and small fragments of the ctenidia) in RNAlater™.

The tissues in RNAlater™ were stored at 2°C for several weeks then frozen in liquid nitrogen and pulverized using a chilled mortar and pestle. We then isolated total RNA using a kit (RNAqueous-4PCR kit, Ambion, Inc.) and performed RT-PCR. We used primer sequences designed by Kier and Schachat (Kier and Schachat, 2008) for the RT-PCR. The forward primer was 5′-AGCTTGGCTGGAAAGAAAGATAA-3′; the reverse primer was 5′-CAGCACCGGCAATTTTACCTT-3′. The primers bracketed the putative alternative RNA splice site identified by Matulef et al. (Matulef et al., 1998) in the funnel retractor muscle of *D. pealeii*. Expression of MHC isoform A or isoform B (*sensu* Matulef et al., 1998) was determined by the lengths of cDNA products, with the isoform A cDNA being 15 bp longer than that of isoform B. Following 40 cycles of PCR amplification, the products were diluted to 20 μg ml^{-1} and then resolved by gel electrophoresis using a 4% high-resolution agarose gel in 1× Tris/Borate/EDTA buffer.

Statistics

For comparison of morphological or muscle mechanics data between two sample populations, we used one-way analysis of variance (ANOVA). For comparisons among multiple groups, we used one-way ANOVA with Tukey's highly significant difference (HSD) post tests. Where indicated in the text, we compared thick filament length and muscle mechanics data from paralarvae collected in this study with similar data from adults reported by Thompson et al. (Thompson et al., 2008) and used here with their permission.

RESULTS

Mantle musculature

The mantle musculature of paralarval and adult *D. pealeii* differed notably in several ways. First, when circular muscle cells of paralarvae were cut transverse to their long axes, their shapes were variable (Fig. 1A,B). Although most muscle cells were roughly triangular or ovoid in cross section with a core of mitochondria (typical of squid mantle muscles), numerous muscle cells with crescent or other unusual cross-sectional shapes, and muscle cells with unequal distributions of mitochondria, were present. The frequency of these fibers relative to 'normal' circular muscle cells ranged from 1:6 to 1:10 among the 19 paralarvae we surveyed. We did not find crescent-shaped circular fibers or fibers with unusual cross-sectional shapes in the circular muscles of adult squid (Fig. 1C,D).

Second, the circular fibers of paralarvae were smaller than those of adults (Table 1). Among paralarvae, the CMP circular muscle fibers had significantly smaller total cross sectional areas than the SMR fibers (P<0.05), and this difference was also seen in the adults (P<0.0001). Both the SMR and CMP fibers of paralarvae had significantly smaller cross sectional areas than their counterparts in the adults (P<0.0001 for both comparisons).

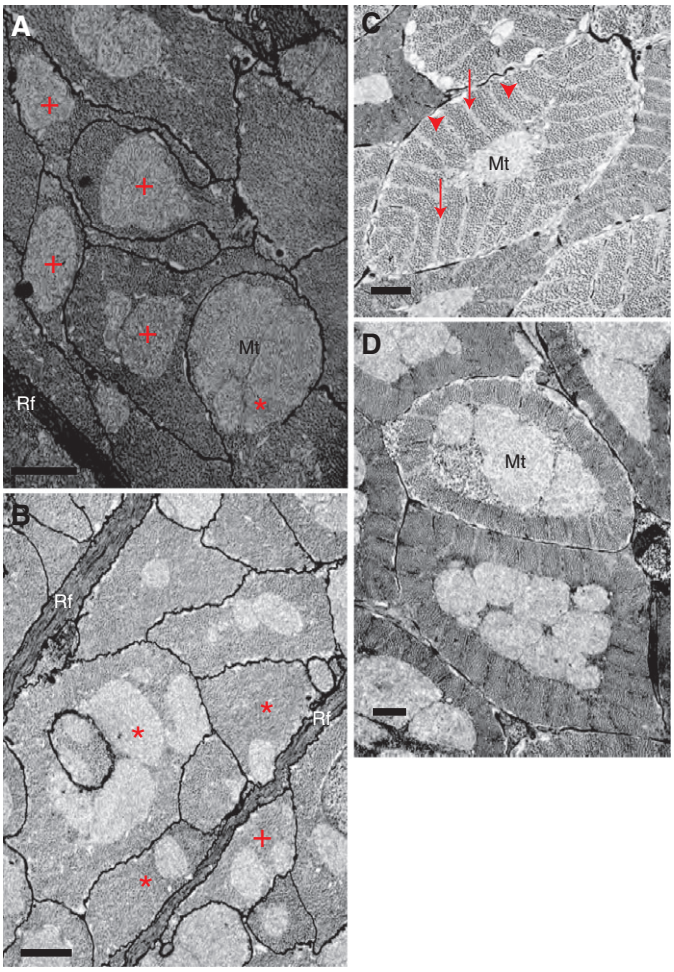

Fig. 1. Transmission electron micrographs of cross sections of the circular muscle fibers of paralarval (A,B) and adult (C,D) *Doryteuthis pealeii*. Cells in A and B with crescentic (+) or other unusual cross sectional profiles, and also cells with unusual distributions of mitochondria (*), are indicated. The central mitochondria-poor (C) and superficial mitochondria-rich (D) circular muscle fibers of adults exhibit alternating light (arrows) and dark bands (arrowheads) that correspond to the I-bands and A-bands, respectively. Note the absence of the alternating bands in the circular fibers of the paralarvae. Mt, mitochondria; Rf, radial muscle fiber. Scale bars, 1 μm.

Third, the general organization of the myofilaments in the cross sections of the circular muscle fibers was different between paralarvae and adults. When sectioned transverse to their long axes,

Table 1. Circular muscle metrics

	Paralarval SMR	Paralarval CMP	Adult SMR	Adult CMP
Cross sectional area (μm^2)	25.7±9.1	14.2±5.4	53.2±12.2	37.5±9.1
Thick filament diameter (nm)	24.2±3	19.8±3	28±3.1	22.7±2.6
Thin:thick filament ratio	8.5±2.1	7.3±2.4	8.3±1.7	5.1±1.1

Comparison of total cross sectional area, thick filament diameter and thin:thick filament ratios between the superficial mitochondria-rich (SMR) and central mitochondria-poor (CMP) circular muscle fibers of paralarval and adult *Doryteuthis pealeii*. The means ± s.d. are listed. The data are from 19 paralarvae and three adults. The thick filament diameter and the thin:thick filament ratio data were obtained from 10 cells in each animal. We measured at least 65 thick filaments in each cell. The cross sectional area data were obtained from the same individuals.

the SMR and CMP muscle fibers of adults showed the banding pattern typical of obliquely striated muscle cells (Figs 1, 2). Briefly, the bands result from alternation of lightly stained regions containing only thin filaments, SR and irregularly spaced dense bodies with more darkly stained regions containing overlapping thick and thin filaments. In the paralarvae, this pattern was not apparent in most of the circular fibers (Fig. 1, Fig. 2A,B). Cross sections of most paralarval circular fibers were composed primarily of regions with both thick and thin filaments, with a few isolated regions composed of either thin filaments or thick filaments only (Fig. 2B). When sectioned parallel to their long axes, the SMR and CMP fibers of both paralarvae and adults exhibited the myofilament arrangements typical of obliquely striated muscle cells but the angle of obliquity of the dense bodies was much greater (i.e. closer to cross striation) in paralarvae than in adults (Figs 3, 4). The angle of obliquity is sensitive to the plane of section (see Rosenbluth, 1965), and thus the mean angle of obliquity must be reported with great caution. Nevertheless, among the hundreds of paralarval and adult muscle cells observed, the means ± s.d. of the 25 lowest angles of obliquity (for SMR and CMP fibers combined) visible in the micrographs were 22.8±2.4 deg. and 4.6±0.8 deg. for paralarvae and adults, respectively. In addition to the difference in angle of obliquity, the dense bodies in some of the paralarval circular fibers did not follow straight trajectories (Fig. 3C). This resulted in adjacent thick filaments being out of the register typically seen in obliquely striated cells. Indeed, some thick filaments within a few circular fibers followed trajectories that were almost perpendicular to the majority of the thick filaments (Fig. 3C).

Fourth, there was a difference in the distribution of SR between paralarvae and adults. In adults, the SR of the circular fibers was well-organized into three zones: a peripheral zone associated with the sarcolemma, a second, central zone surrounding the core of mitochondria, and a third, intramyoplasmic region of flattened tubules located in the plane of the dense bodies that appeared to connect the outer and central zones of SR (Fig. 2). In paralarvae, the outer and central zones of SR were well developed but the intramyoplasmic zone was greatly reduced in some cells or was scattered non-uniformly across the myoplasm (Fig. 2A,B). Whereas in adults the intramyoplasmic SR region was composed primarily of flattened tubules that occasionally swelled into a vesicle, it was composed primarily of large vesicles in the paralarvae, although flattened tubules were present in parts of a small number of paralarval fibers.

Fifth, among paralarvae the thick filaments of the SMR and CMP circular muscle fibers differed slightly in length (P=0.05, Figs 5, 6). During ontogeny, the lengths of the thick filaments of the SMR and CMP fibers increased significantly (P<0.0001 for both comparisons), with the SMR fibers increasing 3.7-fold in length and the CMP fibers 2.5-fold (data for adults from Thompson et al., 2008).

Finally, the thick filament diameter and thin:thick filament ratio changed during ontogeny. Among paralarvae, the CMP thick filaments were significantly (P=0.009) smaller in diameter than the SMR thick filaments. A similar difference was found among adults (P=0.0001) (Table 1). The CMP and SMR thick filaments of paralarvae were significantly smaller in diameter than their counterparts in adults (P=0.037 and P=0.0014 for SMR and CMP fibers, respectively) (Table 1). The thin:thick filament ratio was significantly lower in the CMP fibers of adults compared with the SMR fibers of adults (P=0.05) and with both the CMP and SMR fibers of paralarvae (P<0.05). The thin:thick filament ratios of the SMR and CMP fibers of paralarvae did not differ significantly from each other (P>0.4) (Table 1).

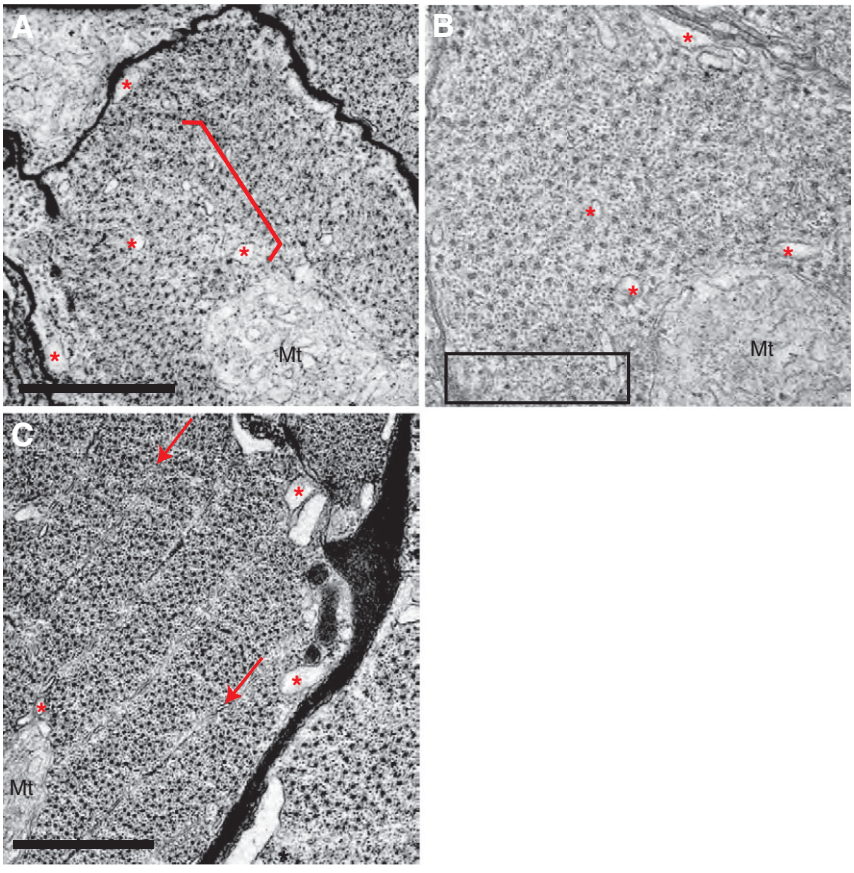

Fig. 2. Transmission electron micrographs of cross sections of the circular muscle fibers of paralarval (A,B) and adult (C) *Doryteuthis pealeii* that highlight differences in sarcoplasmic reticulum (SR) distribution and myofilament arrangement. The circular fibers of both adults and paralarvae have well-developed zones of SR (asterisks in all panels) associated with the sarcolemma and mitochondrial core. The intramyoplasmic SR of paralarvae is composed of vesicles distributed in an apparently haphazard fashion (see bracketed region in A) but in adults it is composed of flattened tubules that appear to connect the peripheral zone of SR with the inner zone of SR (arrows in C). The rectangle in panel B encloses a region with very few thick filaments; the remainder of the cross section of the cell in B is composed of interdigitating thin and thick filaments.
Mt, mitochondria. Scale bars, 1 μm; the rectangle in B is 1 μm in length.

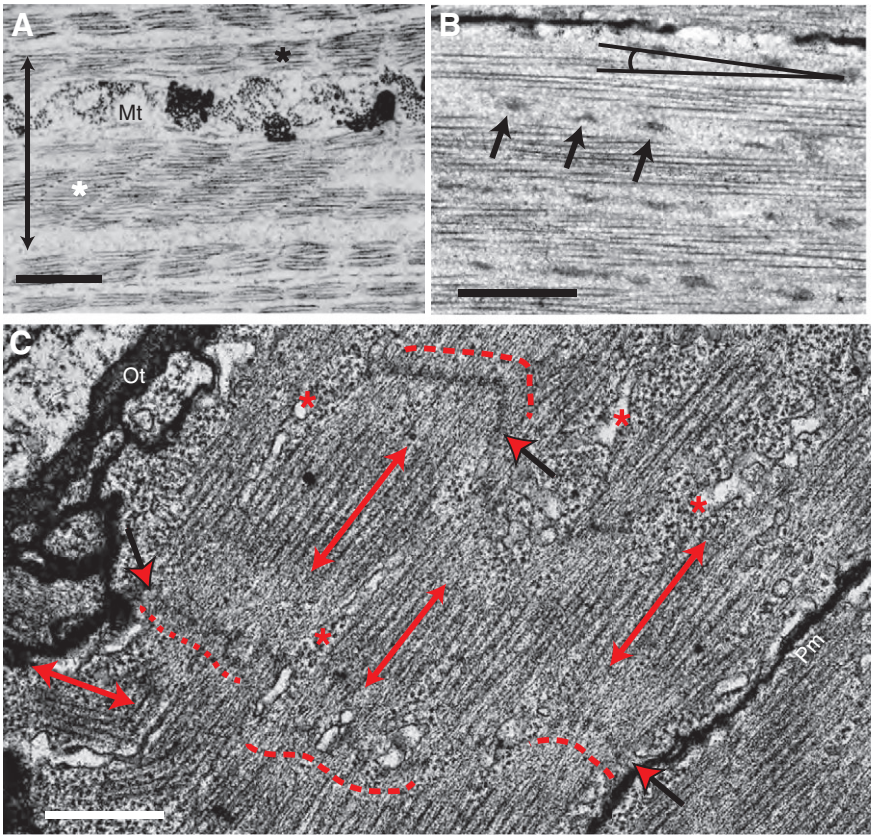

Fig. 3. Transmission electron micrographs of sections parallel to the long axes of the circular fibers of paralarval (A,C) and adult (B) *Doryteuthis pealeii*. (A) Superficial mitochondria-rich (SMR) fiber (width delineated by the double-ended black arrow) that appears cross striated (black asterisk) near the top of the cell but obliquely striated (white asterisk) near the middle and bottom of the cell. Multiple angles of obliquity of the dense bodies are commonly seen in obliquely striated fibers depending on the section plane. The fixative used for this tissue (modified Karnovsky; see Materials and methods for details) did not preserve membranes well; thus, the sarcolemma, the double membrane of the mitochondria (Mt) and the sarcoplasmic reticulum (SR) are difficult to perceive. In addition, black tungsten crystals accumulated in the core of mitochondria. (B) Central mitochondria-poor (CMP) fiber from an adult squid exhibiting the low angle of obliquity (indicated near the top of the cell) of the dense bodies (arrows) typical of both the SMR and CMP obliquely striated muscle fibers of adults. (C) Section of the SMR fiber of a paralarva adjacent to the outer surface of the mantle and the outer tunic (Ot) of collagen fibers. The negative was over-exposed to improve the visibility of the dense bodies (red/black arrows). Note the arrangement of the dense bodies is not linear. Broken red lines above (top of image) and below (bottom of image) indicate the organization of near-by dense bodies. The double-ended red arrows indicate the approximate positions of the thick filaments and their trajectories. Note the trajectories of the thick filaments in the lower left corner of the image. Red asterisks indicate SR. The section plane barely grazes the core of mitochondria of the fiber; thus, the extensive distribution of the inner zone of SR is visible throughout the image. Pm, plasma membrane. Scale bars, 1 μm in A, B and 0.5 μm in C.

Paralarval circular muscle contractile properties

All of the slack tests resulted in tight linear relationships between step length and force recovery time, with the R^2 values for the least-squares linear regressions of all preparations exceeding 0.98 (not shown). For brief tetanus (2 ms pulse width, 50 Hz, 200 ms duration) at 20°C, the mean maximum unloaded shortening velocity (V_{max}) of the paralarval preparations was 9.1 L_0 s^{-1}, where L_0 was the preparation length that generated the peak isometric stress (Fig. 7). V_{max} ranged from 4.3 to 14.8 L_0 s^{-1}.

In the mantle preparations of the paralarvae, the maximum isometric stress in brief tetanus (P_0) was 119±15 mN mm^{-2} pcs with a range of 85–160 mN mm^{-2} pcs.

The temporal aspects of brief tetani are summarized in Table 2.

MHC mRNA expression

Both isoforms of MHC were expressed in the mantles of adults and paralarvae. Isoform 'A' (204 bp) composed at least 90% of the RT-PCR product in all animals, based on relative staining intensity of the bands in the agarose gel (Fig. 8).

DISCUSSION

The fine structure of the circular muscles that provide power for jet locomotion changed in several ways during ontogeny in *D. pealeii*. These include a difference in myofilament organization, the shapes and distribution of SR and the lengths of the thick filaments. All observed changes may have implications for contractile properties of the circular muscles.

Myofilament organization

When cut transverse to their long axes, the CMP and SMR circular muscle fibers of adults showed the alternating band pattern typical of obliquely striated muscle cells (e.g. Kawaguti and Ikemoto, 1957; Rosenbluth, 1965; Rosenbluth, 1968; Ward and Wainwright, 1972; Moon and Hulbert, 1975; Lanzavecchia, 1977) but it was absent from virtually all of the CMP and SMR circular fibers of the paralarvae (Figs 1, 2). The pattern visible from the transverse plane of an obliquely striated cell results from the staggered arrangement of the myofilament lattice proteins (see Rosenbluth, 1965). Thus, a change in the banding pattern suggests a difference in the arrangement of the myofilaments.

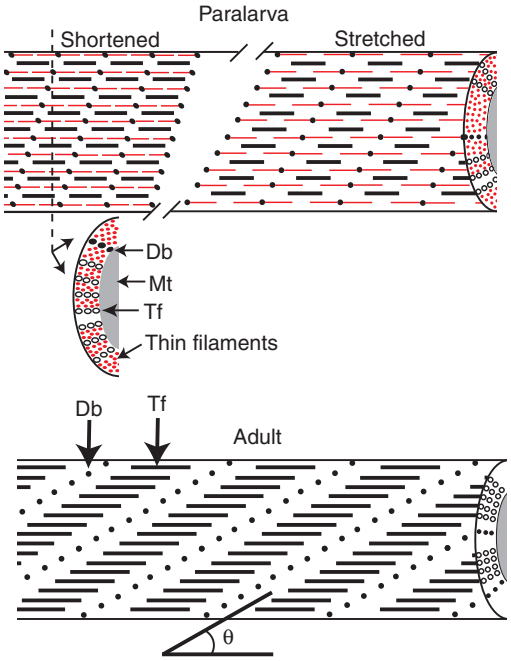

Fig. 4. Schematics to illustrate hypothesized differences in the angle of obliquity (θ) of the dense bodies in the circular muscle fibers of a paralarva (top) and adult (bottom). Dense bodies are indicated as solid black circles, thick filaments as hollow black lines and thin filaments as solid red lines. Both schematics greatly under-represent the numbers of thick and thin filaments. This, in combination with short thick filaments, result in the cross sectional views of the paralarvae exhibiting far fewer A-bands than are actually visible in photomicrographs. The paralarval schematic illustrates the different appearance of cross sections of the fiber when shortened (section plane indicated by the dashed line) or stretched (at far right side of fiber). The greater the angle of obliquity, the greater the proportion of A-bands exhibited in a given cross section of the fiber. The angle of obliquity (22.8 deg. and 4.6 deg. in paralarval and adult circular fibers, respectively) is overestimated in each schematic. Thin filaments were not included in the adult schematic. Db, dense body; Mt, mitochondrial core; Tf, thick filaments.

We propose that the difference in the arrangement of myofilaments between paralarvae and adults results from a greater angle of obliquity of the dense bodies in the circular muscle fibers of paralarvae (Fig. 3). The angle of obliquity increases from 6–12 deg. at rest to 14–18 deg. during contraction in *Loligo* sp. (Hanson and Lowy, 1957; Rosenbluth, 1965; Millman, 1967) and can change with section plane (Rosenbluth, 1965); thus, making comparisons of angle of obliquity between animals is difficult. Nevertheless, the paralarval fibers consistently exhibited substantially higher angles of obliquity even when sections from highly stretched (prior to fixation) paralarval preparations were compared with highly contracted (during fixation) adult preparations. Higher angles of obliquity make it likely that sections transverse to the long axis of the fiber will primarily contain A-bands (i.e. overlapping thick and thin filaments; Fig. 4). Examining sections that are slightly off-axis or sectioning cells that contracted during the fixation process decreases the probability of seeing the banding typical of adults (Fig. 4).

The effect of this change in the organization of the dense bodies on muscle performance is uncertain because the functional implications of oblique striation are not yet clear. Rosenbluth suggested that oblique striation constrains shortening velocity because the friction associated with shearing of the thick filaments may act as a brake (Rosenbluth, 1968). The higher angle of obliquity in paralarval fibers should reduce this friction and result in higher V_{max} relative to otherwise identical fibers that have a lower angle of obliquity.

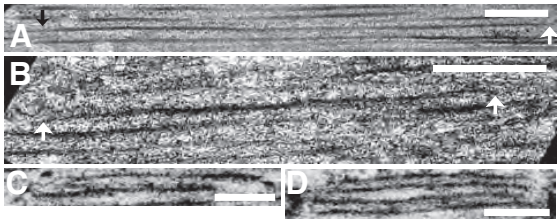

Fig. 5. Transmission electron micrographs showing the ontogeny of thick filament lengths. The thick filaments of adult superficial mitochondria-rich (SMR) (A) and central mitochondria-poor (CMP) (B) fibers were 3.7-fold and 2.5-fold longer, respectively, than the SMR (C) and CMP (D) thick filaments of the paralarvae. The arrows in A and B help delineate one thick filament. Scale bars, 0.5 μm in A, B and 0.25 μm in C, D.

The difference in the arrangement of myofilaments between paralarvae and adults we found is consistent with the photomicrographs of the circular muscle fibers in paralarval and juvenile *D.* (formerly *Loligo*) *opalescens* in Preuss et al. (Preuss et al., 1997), who also noted a difference in the organization of the myofilaments between the SMR fibers and CMP fibers of paralarvae. Preuss and colleagues reported that the myofilaments of paralarvae

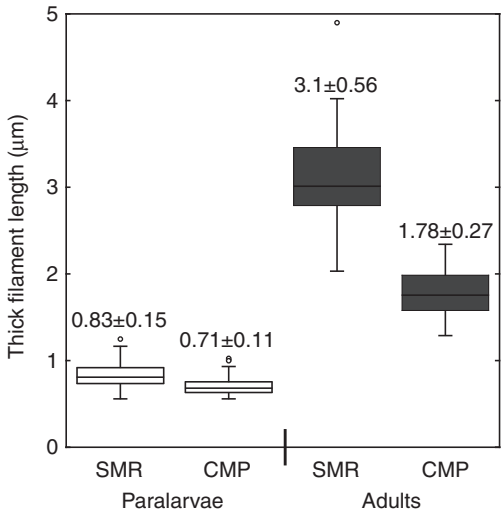

Fig. 6. Thick filament length in the two types of circular muscle fibers in paralarvae and adults. The thick filaments of the adult superficial mitochondria-rich (SMR) fibers were significantly longer than the SMR fibers of paralarvae, and also were significantly longer than the thick filaments of the central mitochondria-poor (CMP) fibers of adults and paralarvae [P<0.0001 for all comparisons; one-way ANOVA with Tukey's highly significant differences (HSD) *post hoc* test]. The thick filaments of the CMP fibers of adults were significantly longer than the thick filaments of both the CMP or SMR fibers of paralarvae (P<0.0001 for all comparisons; one-way ANOVA with Tukey's HSD *post hoc* test). In paralarvae, thick filament lengths differed slightly between the SMR and CMP fibers (P=0.05; one-way ANOVA). The open circles indicate outliers that were at least 1.5 times higher than the interquartile range. The numbers above each box indicate the means ± the s.d. The data for adult *Doryteuthis pealeii* are from Thompson et al. (Thompson et al., 2008), and are used with permission of the authors.

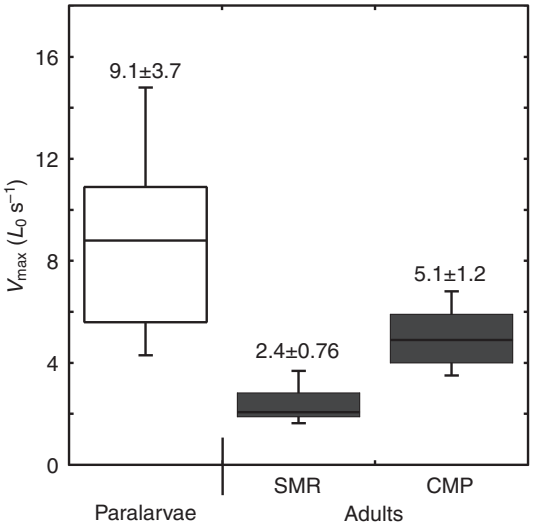

Fig. 7. Boxplot comparing maximum unloaded shortening velocity (V_{max}) in brief tetanus (2 ms pulse width, 50 Hz, 200 ms duration) at 20°C for paralarval and adult *Doryteuthis pealeii* muscle preparations. The paralarval preparations (N=19) included the central mitochondria-poor (CMP) and superficial mitochondria-rich (SMR) circular muscle fibers and intact radial muscle fibers; the adult preparations (N=10) included either the SMR or CMP circular fibers plus the severed fragments of the radial fibers. Paralarval preparations had a significantly higher V_{max} than the CMP fiber preparations of adults (P=0.0007; one-way ANOVA). The numbers above each box indicate the means ± the s.d. L_0 is the preparation length that generated the peak isometric stress. The data for adult *D. pealeii* are from Thompson et al. (Thompson et al., 2008), and are used with permission of the authors.

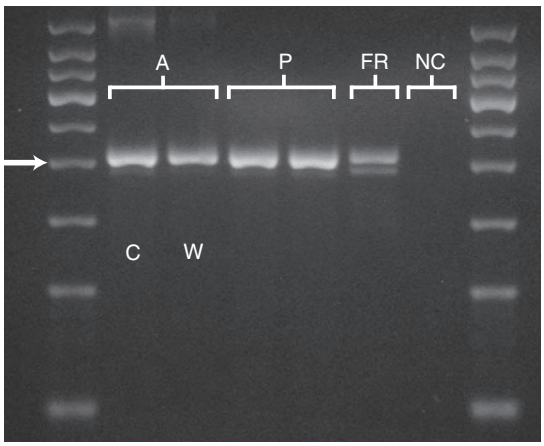

Fig. 8. Photograph of a high resolution 4% agarose gel showing the presence and relative abundance of myosin heavy chain (MHC) isoform A (204 bp) and MHC isoform B (189 bp) in the mantle of adult (A) and paralarval (P) *Doryteuthis pealeii*. The RT-PCR products flank the 200 bp ladder fragment (arrow). In both adult and paralarval mantle, isoform A is present in much greater abundance than isoform B. There were two lanes for the adult mantle: one (C) that included tissue from the central zone of the mantle [i.e. central mitochondria-poor (CMP) circular fibers and radial fibers] and one (W) that included the entire mantle [i.e. both superficial mitochondria-rich (SMR) and CMP circular fibers plus radial fibers]. There were two replicates for the whole muscle preparations of the paralarvae, one lane for a funnel retractor muscle (FR) from an adult *D. pealeii*, and one negative control (NC) lane. The NC contained RNA purified from all three tissues but reverse transcriptase was omitted during the PCR. The adult, paralarval and FR muscle lanes were loaded with 20 μg ml^{-1} of PCR product.

were 'poorly organized' relative to those of adults, and also cautiously suggested that the SMR fibers of paralarval *D. opalescens* were cross-striated (Preuss et al., 1997). We found no evidence to support the suggestion that either the SMR or CMP fibers of *D. pealeii* paralarvae are cross-striated (Figs 2, 3). Indeed, the photomicrograph in Preuss et al. (Preuss et al., 1997) of a paralarval SMR circular muscle fiber seems to display the alternating band pattern typical of obliquely striated fibers.

Table 2. Temporal aspects of the contraction of paralarval and adult mantle muscle fibers

	SMR	CMP	Paralarvae	P
T_L (ms)	4.6±1.4	4.4±1.5	4.0±0.9	0.78
T_P (ms)	143±28.9	143±57.7	126.8±28.1	0.001
T_{50} (ms)	135±28.4	175±98.9	57.4±4.7	<0.001
N	7	10	19	

Comparison of the temporal aspect of the isometric contraction of paralarval and adult mantle muscle preparations in brief tetanus (2 ms pulse, 50 Hz, 200 ms duration). The means ± s.d. are listed. The P values for comparisons between the whole mantle paralarval preparations and the adult central mitochondria-poor (CMP) preparations are listed (one-way ANOVA). There were no differences between adult superficial mitochondria-rich (SMR) and CMP preparations (P>0.4 for all comparisons). T_L, latent period between the first stimulation and rise in force; T_P, time from the rise in force to the peak force; T_{50}, time from peak force to 50% peak force. The SMR and CMP data from adults are from Thompson et al. (Thompson et al., 2008) and are used with permission of the authors.

SR

The ontogenetic differences in intramyoplasmic SR organization and shape (i.e. rounded vesicles in paralarvae *vs* flattened tubules in adults) did not affect the latency between stimulation and the rise of force in the muscle preparations. The delay between stimulation and force rise in the paralarval muscle preparations, 4 ms, was not significantly (P=0.78) shorter than the delay in the CMP (4.4 ms) and SMR (4.6 ms) circular muscle preparations of adult *D. pealeii* reported by Thompson et al. (Thompson et al., 2008). The paralarval preparations achieved peak isometric force significantly faster than both the CMP and SMR fiber preparations of adults (Thompson et al., 2008) (Table 2) but this probably resulted from the lower absolute forces produced by the paralarval preparations. Indeed, the rate of isometric force rise in the paralarval preparations was substantially lower than in either the adult CMP or SMR preparations (data not shown). This probably occurred because the significantly longer thick filaments of the adult circular fibers permitted activation of more cross bridges per unit time. The paralarval muscle preparations relaxed to 50% P_0 about 3 times more rapidly than the CMP preparations of adults (Table 2). We have not identified a mechanism that explains this difference, although it is possible that the rate of calcium return to the SR is greater in paralarvae. Both the faster times to peak force and the time to 50% P_0 suggest that the paralarvae should be able to produce jet pulses with greater frequency than adults, and this is consistent with the results of Bartol et al. (Bartol et al., 2009a) who found shorter jet pulse duration in paralarval *D. pealeii* than in adults (see also Anderson and Grosenbaugh, 2005).

Numerous crescent-shaped cells and cells with unequal distributions of mitochondria were present in the mantles of

paralarvae but not in those of adults. Bone et al. noted crescent-shaped circular muscle cells in the mantle of *Alloteuthis subulata* and suggested that these represented early stages of new fibers formed from cell division (Bone et al., 1981). The frequent occurrence of such cells in the mantle of paralarvae in which growth and, presumably, rates of cell division are high (Moltschaniwskj, 1994; Moltschaniwskj, 1995; Moltschaniwskj, 1997), lends support to the hypothesis of Bone et al. (Bone et al., 1981).

Thick filament length

There was a significant increase in the lengths of the thick myofilaments of both the CMP and SMR circular muscle fibers (Figs 3, 5) through ontogeny from paralarvae to adults. This increase was similar to that found in the CMP and SMR fibers of another loliginid squid, *S. lessoniana* (Thompson and Kier, 2006), and suggests that such changes may be common among squids. The ontogenetic increase in the thick filament lengths of the circular muscles of *D. pealeii* and *S. lessoniana* are not unique among cephalopod muscles (Kier, 1996), and Kier and colleagues have suggested that loliginid squids modulate muscle contractile properties by altering thick filament length alone (Kier, 1985; Kier, 1996; Kier and Schachat, 1992; Kier and Curtin, 2002; Thompson and Kier, 2006; Kier and Schachat, 2008; Thompson et al., 2008).

Implications of thick filament length ontogeny for muscle function

The shortening velocity of striated muscles, including the obliquely striated circular muscles, depends on a variety of factors: the lengths of the thick filaments and sarcomeres, the load on the muscle and the rate of cross-bridge cycling (e.g. Bárány, 1967; Josephson, 1975). In general, thick filament length is inversely proportional to unloaded shortening velocity and directly proportional to peak isometric stress (Millman, 1967; Josephson, 1975; Kier and Curtin, 2002).

In adult *D. pealeii*, there is a strong correlation between thick filament length and contractile properties in the SMR and CMP circular muscle fibers (Thompson et al., 2008). The mean thick filament length of the adult SMR fibers (3.12 μm) is 1.75-fold greater than that of the adult CMP fibers (1.78 μm) (Thompson et al., 2008). Thus, if other aspects of the two fiber types are the same, and if the relationship between thick filament length and isometric stress is linear, the P_0 of the SMR fibers should be 1.75 times greater than the P_0 of the CMP fibers. Thompson et al. (Thompson et al., 2008) found that the P_0 of the adult SMR fibers was approximately 1.5 times greater; correcting for differences in the size of the core of mitochondria between the two fiber types resulted in a P_0 that was about 2 times greater. By similar reasoning, the V_{max} of the adult SMR fibers should be 1.75 times slower than the CMP fibers, and it was approximately 2 times slower (Thompson et al., 2008).

Assuming that other aspects of the circular muscles do not change during ontogeny, we therefore hypothesized that the circular muscles of paralarvae produce lower peak isometric stresses and higher unloaded shortening velocities than those of adults. Before analyzing this hypothesis in light of our results, we first discuss the limitations of our mechanical testing methods.

Limitations of the mechanical testing methods

The thin, deformable mantles of paralarvae thwarted our attempts to investigate the contractile properties of preparations composed solely of CMP or solely of SMR circular fibers. Thus, we studied mantle preparations that contained both types of circular muscle cells in addition to radial fibers. Electrical stimulation of the paralarval muscle preparations probably resulted in contraction of all muscle fibers, and this complicates the comparisons of muscle contractile properties. Nevertheless, several factors support the validity of our experimental approach. First, the thick filaments of the CMP and SMR fibers of paralarval *D. pealeii* are roughly similar in length (Figs 3, 5). If, as our results and those from other studies suggest (Kier and Curtin, 2002; Thompson et al., 2008), the contractile properties of cephalopod obliquely striated muscles are determined largely by thick filament length, then the contractile properties of paralarval CMP and SMR circular muscle fibers are likely to be similar. Nonetheless, our experimental design masked any differences in contractile properties between the two fiber types.

Second, the radial muscle fibers are antagonists to the circular fibers and their activity therefore may have decreased both the speed of shortening and the peak isometric stress of the circular muscle fibers. We attempted to estimate the magnitude of this error in paralarvae as follows. We made mantle muscle preparations from two small adult *D. pealeii* (90 mm and 110 mm DML) that had intact radial fibers and both SMR and CMP circular fibers. We then measured the contractile properties of these preparations using the same methods described earlier in this paper. By comparing the results with those of Thompson et al. (Thompson et al., 2008) for SMR and CMP preparations in which the radial fibers were severed and, therefore, inactivated, we were able to estimate the error introduced by having intact radial muscle fibers in the preparations. The mean V_{max} from the two intact adult preparations was 4.5±0.7 $L_0\,s^{-1}$, about 12% lower than the mean V_{max} for the CMP preparations of adult squid (Thompson et al., 2008). The mean P_0 for the adult whole mantle preparations was 306±15 mN mm^{-2} pcs, about 8.5% less than the value for the isolated SMR preparations from adults (Thompson et al., 2008). This suggests that our muscle mechanics data underestimate the true V_{max} and P_0 by 8–12%.

Third, Lowy and Millman measured the contractile properties of the funnel retractor muscles of the octopuses *Octopus vulgaris* and *Eledone moschata* and the cuttlefish *Sepia officinalis* (Lowy and Millman, 1962). The funnel retractor is similar to the mantle in that (1) it is supported by a muscular hydrostat with muscle fibers oriented in two directions – parallel and transverse to the long axis of the muscle; (2) the parallel and transverse fibers are antagonists; and (3) the parallel fibers compose the majority of the muscle, just as the circular fibers compose the majority of the mantle musculature (Kier and Thompson, 2003). Lowy and Millman measured the contractile properties of the parallel fibers in intact funnel retractor muscles and preparations in which they pared the muscle down its long axis, thereby severing the transverse fibers (Lowy and Millman, 1962). They found no differences in the properties of the two types of preparations with the exception that the pared preparations produced higher forces per unit cross sectional area.

Despite these reassurances we nevertheless emphasize that the V_{max} and P_0 data we report for paralarvae are conservative estimates.

Ontogeny of circular muscle contractile properties

Even with the conservative estimate of unloaded shortening velocity in the paralarvae, the data support the hypothesis that V_{max} is lower in adult SMR and CMP circular fibers than in the paralarval circular fibers. The mean V_{max} of the SMR and CMP fibers of adult *D. pealeii* in brief tetanus was 2.4 and 5.1 $L_0\,s^{-1}$, respectively, where L_0 was the preparation length that yielded the highest force (Thompson et al., 2008). The mean V_{max} of the adult SMR and CMP preparations was 3.8- and 1.8-fold lower, respectively, than the V_{max} of the paralarval preparations (9.1 $L_0\,s^{-1}$).

The difference in V_{max} between paralarvae and adults was less than that predicted based solely on the ontogenetic increase in thick

filament length. The thick filaments of adult CMP fibers were 2.5 times longer than those of paralarvae, yet the V_{max} of adult CMP fibers was only 1.8 times lower (Thompson et al., 2008). Several variables confound this comparison. First, paralarval preparations were composed of intact circular and radial muscle fibers whereas the radial fibers were severed in the adult preparations (Thompson et al., 2008). If the whole mantle preparations of adults described above provide a realistic effect of the radial fibers on V_{max}, then we need to correct the V_{max} of paralarvae by 12%. Doing so raises the V_{max} to 10.2 L_0 s^{-1} and increases the speed of shortening of the paralarval preparations relative to adult CMP preparations to 2-fold. Second, the SMR fibers of the paralarvae had thick filament lengths that were 1.16 times longer than the CMP fibers (Figs 3, 5). If V_{max} scales linearly with thick filament length in the paralarvae, the slightly slower SMR fibers may have added a load to the CMP fibers; thus, lowering V_{max}. Third, the paralarvae had numerous crescent-shaped and other unusually shaped circular muscle fibers, and the ratio of these to 'normal' fibers varied from 1:6 to 1:10 among the paralarval preparations. If these cells did not generate as much force per unit cross section as the 'normal' circular fibers, the greater the ratio of these cells in a preparation, the greater the load on the 'normal' cells and, therefore, the lower the V_{max}. Indeed, there was greater variation in the paralarval than in the adult preparations, with V_{max} ranging from 4.3 to 14.8 L_0 s^{-1} (Fig. 5) in paralarvae. Although undetected damage to the preparations during dissection may account for some of this variation, we believe that most of it reflects natural variation in the contractile properties of the circular muscles. Paralarvae in the lab differed greatly in their swimming performance, and differences in the contractile properties of the mantle musculature, among other factors, contributed to this variation in locomotion.

Some of the paralarvae had a V_{max} that was nearly 3-fold higher than that of adults. Because thick filament length was relatively uniform among all the paralarvae (Figs 3, 5), this calls into question the notion that thick filament length alone explains the ontogeny of V_{max}. The passive tension in the paralarval and adult CMP preparations was minimal at L_0 (data not shown). Thus, it is unlikely that elastic recoil during the slack tests contributed to the V_{max} data we present.

The P_0 we recorded for the paralarval preparations was much lower than that reported by Thompson et al. (Thompson et al., 2008) for the SMR and CMP preparations of adult *D. pealeii*. It is, however, very similar to the P_0 (131±56 mN mm^{-2} psc) of the transverse muscle fibers of the tentacles of adult *D. pealeii* (Kier and Curtin, 2002). The tentacle muscle fibers are cross-striated (Kier, 1982) and, like the SMR and CMP circular fibers of paralarvae, have short (0.8 μm) thick filaments (Kier and Curtin, 2002).

Alternative splicing of the MHC gene

The dimensions of the myofilaments are but one factor that may affect the contractile properties of the SMR and CMP muscle fibers. The contractile properties of striated muscle fibers may be altered in a variety of ways, including, but not limited to, expression of different isoforms of the myofilament lattice proteins (e.g. Kendrick-Jones et al., 1976; Sweeney et al., 1988; Marden et al., 1998; Schiaffino and Reggiani, 1996; Toniolo et al., 2007). In contrast to mammals, in which nine MHC genes are expressed in skeletal and cardiac muscle and 38 orthologs of MHC have been putatively identified (Maccatrozzo et al., 2007), only a single MHC gene has been identified to date in loliginid squid but it has two splice variants ('A' and 'B') (Matulef et al., 1998). The splice site occurs along one of the nucleotide binding regions of the protein, so the two splice variants may well differ in their ATPase activity (Matulef et al., 1998).

Both predicted splice variants of the MHC gene were expressed in the mantles of paralarvae and adults. The results of the RT-PCR are consistent with the interpretation that isoform A is expressed in much higher levels than isoform B. Within the mantle of an adult, there is no evidence to suggest different expression patterns of the two isoforms between the central zone alone (i.e. the CMP fiber layer and the radial fibers) and the whole mantle (i.e. the CMP and SMR circular fibers and the radial fibers). Thus, our results are consistent with the hypothesis that the contractile properties of the circular muscles are modulated *via* changes in thick filament length, and not *via* changes in the molecular species of MHC present.

In their study of the transverse muscle fibers of the arms and tentacles of *D. pealeii*, Kier and Schachat found no changes in the expression of MHC between the two appendages (Kier and Schachat, 1992) and, similar to our results, that isoform A is expressed at higher levels (>90%) than isoform B in both appendages (Kier and Schachat, 2008).

As striking as these results are, we nevertheless cannot state firmly that changes in the biochemistry of the circular muscles do not underlie the significant ontogenetic decline in V_{max}. Work to sequence the genome of *D. pealeii* is far from complete. Although cephalopods may not have the same diversity of MHC genes as vertebrates and arthropods, additional squid MHC genes may yet be discovered. In addition, expression of different isoforms of other myofilament lattice proteins (e.g. Kendrick-Jones et al., 1976; Sweeney et al., 1988; Lowey et al., 1993; Marden et al., 1998; Schiaffino and Reggiani, 1996; Toniolo et al., 2007) during ontogeny may affect the contractile properties of the circular fibers.

It is important to note that we do not know where each isoform of MHC is expressed in the mantle or any of the other tissues we examined. The isoforms may be co-expressed within a single muscle fiber, as sometimes occurs in the striated muscle fibers of mammals (Staron and Pette, 1987; Schiaffino and Reggiani, 1996) and the nematode *Caenorhabditis elegans* (Miller et al., 1986), or a single muscle fiber may express only one of the isoforms, as is often the case in the striated fibers of mammals and fish (Goldspink, 1998). We do not know if the two isoforms of MHC confer different contractile properties on the muscles in which they are expressed. It is quite possible that the two isoforms differ in ATPase activity given that the alternative splice site falls along one of the regions of the MHC gene that codes for the putative nucleotide binding region of the protein (Matulef et al., 1998), and changes in the structure of this region can affect ATP turnover rates in the MHC isoforms of scallops (Perreault-Micale et al., 1996). Despite these important gaps in knowledge, the molecular data we present do not illustrate an obvious difference in isoform expression pattern during ontogeny.

Linking mantle muscle ultrastructure with jetting performance

If the mechanics of the circular muscles change during ontogeny, an interesting question is raised: is a change in circular muscle mechanics associated with ontogenetic changes in jet dynamics or jet propulsive efficiency? The answer is that yes, indeed, jet locomotion changes during ontogeny in a manner consistent with predictions based on the concurrent changes in mantle muscle structure and function we report. The rationale for this statement is provided below.

Many paralarval squids, including *D. pealeii*, are planktonic and appear to spend much of their time maintaining vertical position in the water column using vertically directed jets (Boletzky, 1974;

Zeidberg and Hamner, 2002). To increase speed, as they would for prey capture or to undergo daily vertical migrations (Zeidberg and Hamner, 2002), paralarval *D. pealeii* increase the amplitude, but not the rate, of mantle contraction (Bartol et al., 2009a). In other words, paralarvae employ a relatively constant jet velocity across the range of speeds (5–27 DML s^{-1}) considered by Bartol et al. (Bartol et al., 2009a), varying speed by altering the total mass of water expelled per mantle contraction. By contrast, adult *D. pealeii* increase jetting speed by adjusting both the rate and amplitude of mantle contraction (Anderson and Grosenbaugh, 2005) (J.T.T. and K. R. Taylor, unpublished). Increasing the rate of mantle contraction requires application of greater pressure to the water in the mantle cavity, and this pressure is derived, ultimately, from active stress produced by the circular muscle fibers. The short thick filaments of the paralarval SMR and CMP circular fibers result in significantly lower peak stress production, and this limits the ability of paralarvae to produce high mantle cavity pressures.

This effect can be seen more clearly if the mantle is modeled as a pressurized circular cylinder. In a thin-walled cylinder, the relationship between the stress in the wall, the pressure in the mantle cavity and the radius of the mantle is given by a variation of Laplace's Law (Fung, 1994):

$$p = \sigma t / r_i \quad (1)$$

where σ is the mean circumferential stress in the mantle wall (i.e. the stress generated by the circular muscle fibers), r_i is the radius of the inner edge of the mantle wall, t is the thickness of the mantle wall and p is the internal pressure (i.e. the pressure in the mantle cavity). We substituted measured values of mantle radius, mantle wall thickness and the peak isometric stress generated by the circular muscles of paralarval (119 mN mm^{-2}) and the CMP circular fibers of adult *D. pealeii* (216 mN mm^{-2}) (Thompson et al., 2008). We predict that a paralarval *D. pealeii* could generate a peak mantle cavity pressure of 12.7 kPa during jetting whereas an adult could produce a peak pressure of nearly 58 kPa. These predicted peak pressures would never be realized *in vivo* because the circular muscles produce much lower stresses during the isotonic shortening required of jetting (Milligan et al., 1997). In addition, Eqn 1 is for a closed cylinder, and fluid expelled from the open funnel aperture of a squid will prevent pressures from reaching those theoretical maxima. Nevertheless, the significantly lower peak isometric stress of the paralarval circular muscles imposes a constraint on thrust production (see Thompson and Kier, 2002) (J.T.T., P.S.K. and I.K.B., unpublished) and the strategies used to increase swimming speed (see Bartol et al., 2009a).

Paralarval squid swim in an intermediate Reynolds number (*Re*) fluid regime in which inertial forces dominate fluid dynamic drag but viscous forces are considerable. Within this environment, they utilize an intermittent or pulsed jet for propulsion. Squids form a jet pulse by first expanding the mantle radially and filling the mantle cavity. Once the mantle cavity is full, the circular muscles contract, thereby increasing the pressure in the mantle cavity and driving water out of the mantle cavity through the funnel. Repetition of this cycle results in a pulsed jet. Studies of mechanically generated pulsed jets at high (>1000) *Re* issuing into quiescent fluid have demonstrated the important role played by the formation of vortex rings at the leading edge of each jet pulse. Vortex rings provide additional thrust through nozzle exit over-pressure, i.e. fluid pressure above the local ambient pressure during jet ejection, which develops as additional ambient fluid downstream is accelerated by entrainment and added mass effects during ring formation (Krueger and Gharib, 2003; Krueger and Gharib 2005; Choutapalli, 2006). As a result of the additional input through over-pressure, pulsed jets can produce substantially more thrust than equivalent steady jets (Krueger and Gharib, 2005). Recent results have shown that paralarval *D. pealeii* also develop vortex-ring-like structures during jetting and hence may benefit from enhanced thrust that is useful for combating the drag challenges experienced at intermediate *Re* (Bartol et al., 2008; Bartol et al., 2009a).

To capitalize on over-pressure benefits provided by pulsing, it is essential to use short pulses. In particular, the ratio of the length of the ejected plug of fluid (L) to the nozzle diameter (D) should be small enough so that isolated vortex rings are formed with each pulse. If L/D is too large, the vortex ring will pinch off from the generating jet (Gharib et al., 1998) and the relative contribution of over-pressure related to the vortex ring formation will decline as the remainder of the pulse is ejected as a relatively steady jet (Krueger and Gharib, 2003). Not only do short jet pulses amplify the thrust benefit of pulsing but recent results from juvenile and adult *L. brevis* (Bartol et al., 2009b) and 'Robosquid' (Nichols et al., 2008) have shown that propulsive efficiency can also be improved by relying on short jet pulses during pulsed jetting. Indeed, paralarval *D. pealeii* seem to rely almost exclusively on relatively short jet pulses, which appears to be a contributing factor leading to their remarkably high propulsive efficiencies despite the intermediate *Re* at which they swim (Bartol et al., 2008; Bartol et al., 2009a).

In the context of swimming at intermediate *Re* and the considerable benefit pulsed jetting with short jet pulses appears to provide, the present results of increased V_{max} and short circular muscle relaxation times in paralarval *D. pealeii*, as compared with their adult counterparts, is particularly intriguing. Although we do not know the load on the circular musculature during jetting or how it scales with body size, the significantly higher V_{max} of the paralarvae undoubtedly contributes to their ability to produce the short jet pulses that are important for maintaining high propulsive efficiency. In addition, the higher V_{max} and shorter relaxation times may also facilitate the high jet pulsing frequencies that are often observed in paralarvae (I.K.B. and J.T.T., personal observation) (Bartol et al., 2009a), which allow for more continuous swimming and shorter coasting phase durations within each jet cycle. The ability to swim more continuously with short periodic refill periods during jet cycles is an important consideration at intermediate *Re* where the considerable viscosity inhibits coasting.

High jet propulsive efficiency actually may be more important for paralarvae than older life-history stages because their fins play such a minor role in propulsion relative to the contributions of the highly efficient fins of juveniles and adults (Bartol et al., 2008), requiring paralarvae to rely more heavily on their jet for propulsion. Thus, ultrastructural modifications of the circular muscle fibers over ontogeny may have evolved in response to the need for the rapid mantle contractions and short jet periods that lead to high propulsive efficiency.

LIST OF ABBREVIATIONS

CMP	central mitochondria-poor circular muscle fibers
D	diameter of jet nozzle
DML	dorsal mantle length
L	length of the ejected plug of fluid
L_0	muscle preparation length that produced the peak isometric stress in brief tetanus
MHC	myosin heavy chain
p	pressure inside the mantle cavity
P_0	maximum isometric stress in brief tetanus
pcs	physiological cross sectional area

r_i	radius of the inner surface of the mantle
Re	Reynolds number
RT-PCR	reverse transcriptase-polymerase chain reaction
SMR	superficial mitochondria-rich circular muscle fibers
SR	sarcoplasmic reticulum
t	thickness of the mantle wall
V_{max}	maximum unloaded shortening velocity
σ	isometric stress produced by the circular muscles

ACKNOWLEDGEMENTS

We thank the staff of the Darling Marine Center (DMC), especially Mr Tim Miller and Ms Linda Healy, for help in finding and housing squid, and also for lab space and housing for J.T.T. and A.B. We also thank Oluwarotimi Adesina, Stephen Chorney and Karen Ross for help in maintaining squid at the DMC. We thank Dr Robert Jinks for assistance with the electron microscopy and sharing the ultramicrotomes in his lab. The research was supported by National Science Foundation grant IOS-0446081 to J.T.T., I.K.B. and P.S.K., and start-up funds from Franklin & Marshall College.

REFERENCES

Abramoff, M. D., Magelhaes, P. J. and Ram, S. J. (2004). Image processing with ImageJ. *Biophotonics Int.* **11**, 36-42.
Anapol, F. and Herring, S. W. (1989). Length–tension relationships of masseter and digastric muscles of minature swine during ontogeny. *J. Exp. Biol.* **143**, 1-16.
Anderson, E. J. and Grosenbaugh, M. A. (2005). Jet flow in steadily swimming adult squid. *J. Exp. Biol.* **208**, 1125-1146.
Bandman, E. (1985). Myosin isoenzyme transitions in muscle development, maturation and disease. *Int. Rev. Cytol.* **97**, 97-131.
Bárány, M. (1967). ATPase activity of myosin correlated with speed of muscle shortening. *J. Gen. Physiol.* **50**, 197-218.
Bartol, I. K. (2001). Role of aerobic and anaerobic circular mantle muscle fibers in swimming squid: electromyography. *Biol. Bull.* **204**, 59-66.
Bartol, I. K., Krueger, P. S., Thompson, J. T. and Stewart, W. J. (2008). Swimming dynamics and propulsive efficiency of squids throughout ontogeny. *Int. Comp. Biol.* **48**, 720-733.
Bartol, I. K., Krueger, P. S., Stewart, W. J. and Thompson, J. T. (2009a). Wake dynamics of squid paralarvae at intermediate Reynolds numbers. *J. Exp. Biol.* **212**, 1506-1518.
Bartol, I. K., Krueger, P. S., Stewart, W. J. and Thompson, J. T. (2009b). Hydrodynamics of pulsed jetting in juvenile and adult brief squid *Lolliguncula brevis*: evidence of multiple jet 'modes' and their implications for propulsive efficiency. *J. Exp. Biol.* **212**, 1889-1903.
Biewener, A. A., Konieczynski, D. D. and Baudinette, R. V. (1998). *In vivo* muscle force-length behavior during steady-speed hopping in tammar wallabies. *J. Exp. Biol.* **201**, 1681-1694.
Boletzky, S. v. (1974). The 'larvae' of Cephalopoda: A review. *Thalassia Jugoslavica* **10**, 45-76.
Bone, Q., Pulsford, A. and Chubb, A. D. (1981). Squid mantle muscle. *J. Mar. Biol. Assoc. UK* **61**, 327-342.
Bone, Q., Brown, E. R. and Usher, M. (1995). The structure and physiology of cephalopod muscle fibres. In *Cephalopod Neurobiology* (ed. N. J. Abbott, R. Williamson and L. Maddock), pp. 89-101. New York: Oxford University Press.
Bower, J. R., Sakurai, Y., Yamamoto, J. and Ishii, H. (1999). Transport of the ommastrephid squid *Todarodes pacificus* under cold-water anesthesia. *Aquaculture* **170**, 127-130.
Bozzola, J. J. and Russell, L. D. (1992). *Electron Microscopy. Principles and Techniques for Biologists*. Boston: Jones and Bartlett.
Choutapalli, I. M. (2006). An experimental study of a pulsed jet ejector. PhD Thesis, Florida State University, Tallahassee, FL, USA.
Edman, K. A. P. (1979). The velocity of unloaded shortening and its relation to sarcomere length and isometric force in vertebrate muscle fibres. *J. Physiol.* **291**, 143-159.
Elemans, C. P. H., Spierts, I. L. Y., Muller, U. K., van Leeuwen, J. L. and Goller, F. (2004). Superfast muscles control dove's trill. *Nature* **431**, 146.
Etnier, S. A., Dearolf, J. L., McLellan, W. A. and Pabst, D. A. (2008). Postural role of lateral axial muscles in developing bottlenose dolphins (*Tursiops truncates*). *Proc. R. Soc. Lond., B, Biol. Sci.* **271**, 909-918.
Fitzhugh, G. H. and Marden, J. H. (1997). Maturational changes in troponinT expression, calcium sensitivity, and twitch contraction kinetics in dragonfly flight muscle. *J. Exp. Biol.* **200**, 1473-1482.
Full, R. J., Stokes, D. R., Ahn, A. N. and Josephson, R. K. (1998). Energy absorption during running by leg muscles in a cockroach. *J. Exp. Biol.* **201**, 997-1012.
Fung, Y. C. (1994). *A First Course in Continuum Mechanics for Physical and Biological Scientists and Engineers*, 3rd edn. Englewood Cliffs, NJ: Prentice Hall.
Gauthier, G. F., Lowey, S. and Hobbs, A. (1978). Fast and slow myosin in developing muscle fibres. *Nature* **274**, 27-29.
Gharib, M., Rambod, E. and Shariff, K. (1998). A universal time scale for vortex ring formation. *J. Fluid Mech.* **360**, 121-140.
Gilly, W. F., Hopkins, B. and Mackie, G. O. (1991). Development of giant motor axons and neural control of escape responses in squid embryos and hatchlings. *Biol. Bull.* **180**, 209-220.
Goldspink, G. (1968). Sarcomere length during the post-natal growth of mammalian muscle fibre. *J. Cell Sci.* **6**, 593-603.
Goldspink, G. (1983). Alterations in myofibril size and structure during growth, exercise, and changes in environmental temperature. In *Handbook of Physiology. Section* **10***, Skeletal Muscle* (ed. L. D. Peachey), pp. 539-554. Bethesda, MD: American Physiological Society.
Goldspink, G. (1998). Selective gene expression during adaptation on muscle in response to different physiological demands. *Comp. Biochem. Physiol. B.* **120**, 5-15.
Goldspink, G. and Ward, P. S. (1979). Changes in rodent muscle fibre types during post-natal growth, undernutrition and exercise. *J. Physiol.* **296**, 453-469.
Gondret, F., Lefaucheur, L., D'Albis, A. and Bonneau, M. (1996). Myosin isoform transitions in four rabbit muscles during postnatal growth. *J. Muscle Res. Cell Motil.* **17**, 657-667.
Gosline, J. M., Steeves, J. D., Harman, A. D. and DeMont, M. E. (1983). Patterns of circular and radial mantle muscle activity in respiration and jetting of the squid *Loligo opalescens*. *J. Exp. Biol.* **104**, 97-109.
Greer-Walker, M. (1970). Growth and development of skeletal muscle fibres of cod (*Gadus morhua* L.). *J. Cons. Perm. Int. Explor. Mer.* **33**, 228-244.
Hanson, J. and Lowy, J. (1957). Structure of smooth muscles. *Nature* **180**, 906-909.
Herrel, A., Meyers, J. J., Timmermans, J. P. and Nishikawa, K. C. (2002). Supercontracting muscle: producing tension over extreme muscle lengths. *J. Exp. Biol.* **205**, 2167-2173.
Hoyle, G., McAlear, J. H. and Selverston, A. (1965). Mechanism of supercontraction in a striated muscle. *J. Cell Biol.* **26**, 621-640.
Josephson, R. K. (1975). Extensive and intensive factors determining the performance of striated muscle. *J. Exp. Zool.* **194**, 135-154.
Kawaguti, S. and Ikemoto, N. (1957). Electron microscopy of the smooth muscle of a cuttlefish, *Sepia esculenta*. *Biol. J. Okayama Univ.* **3**, 196-208.
Kendrick-Jones, J., Szentkiralyi, E. M. and Szent-Györgyi, A. G. (1976). Regulatory light chains in myosins. *J. Mol. Biol.* **104**, 747-775.
Kier, W. M. (1982). The functional morphology of the musculature of squid (Loliginidae) arms and tentacles. *J. Morphol.* **172**, 179-192.
Kier, W. M. (1985). The musculature of squid arms and tentacles: ultrastructural evidence for functional differences. *J. Morphol.* **185**, 223-239.
Kier, W. M. (1996). Muscle development in squid: ultrastructural differentiation of a specialized muscle fiber type. *J. Morphol.* **229**, 271-288.
Kier, W. M. and Curtin, N. A. (2002). Fast muscle in squid (*Loligo pealei*): contractile properties of a specialized muscle fibre type. *J. Exp. Biol.* **205**, 1907-1916.
Kier, W. M. and Schachat, F. H. (1992). Biochemical comparison of fast- and slow-contracting squid muscle. *J. Exp. Biol.* **168**, 41-56.
Kier, W. M. and Schachat, F. H. (2008). Muscle specialization in the squid motor system. *J. Exp. Biol.* **211**, 164-169.
Kier, W. M. and Thompson, J. T. (2003). Muscle arrangement, function and specialization in recent coleoids. *Berl. Paläobiologische Abh.* **3**, 141-162.
Krueger, P. S. and Gharib, M. (2003). The significance of vortex ring formation to the impulse and thrust of a starting jet. *Phys. Fluid.* **15**, 1271-1281.
Krueger, P. S. and Gharib, M. (2005). Thrust augmentation and vortex ring evolution in a fully-pulsed jet. *AIAA J.* **43**, 792-801.
Lanzavecchia, G. (1977). Morphological modulations in helical muscles (Aschelminthes and Annelida). *Int. Rev. Cytol.* **51**, 133-186.
Lowy, J. and Millman, B. M. (1962). Mechanical properties of smooth muscles of cephalopod molluscs. *J. Physiol.* **160**, 353-363.
Lowey, S., Waller, G. S. and Tyrbus, K. M. (1993). Skeletal muscle myosin light chains are essential for physiological speeds of shortening. *Nature* **365**, 454-456.
Lutz, G. J. and Rome, L. C. (1994). Built for jumping: the design of frog muscular system. *Science* **263**, 370-372.
Maccatrozzo, L., Caliaro, F., Toniolo, L., Patruno, M., Reggiani, C. and Mascarello, F. (2007). The sarcomeric myosin heavy chain gene family in the dog: Analysis of isoform diversity and comparison with other mammalian species. *Genomics* **89**, 224-236.
Marceau, F. (1905). Recherches sur la structure des muscles du manteau des Céphalopodes en rapport avec leur mode du contraction. *Trav. Lab. Soc. Sc. Arachon. Ann.* **8**, 48-65.
Marden, J. H., Fitzhugh, G. H. and Wolf, M. R. (1998). From molecules to mating success: integrative biology of muscle maturation in a dragonfly. *Am. Zool.* **38**, 528-544.
Marsh, R. L. and Olson, J. M. (1994). Power output of scallop adductor muscle during contractions replicating the *in vivo* mechanical cycle. *J. Exp. Biol.* **193**, 139-156.
Matulef, K., Sirokmán, K., Perreault-Micale, C. and Szent-Györgyi, A. G. (1998). Amino-acid sequence of squid myosin heavy chain. *J. Muscle Res. Cell Motil.* **19**, 705-712.
Messenger, J. B., Nixon, M. and Ryan, K. P. (1985). Magnesium chloride as an anaesthetic for cephalopods. *Comp. Biochem. Physiol.* **82C**, 203-205.
Miller, D. M., Stockdale, F. E. and Karn, J. (1986). Immunological identification of the genes encoding the four myosin heavy chain isoforms of *Caenorhabditis elegans*. *Proc. Natl. Acad. Sci. USA* **83**, 2305-2309.
Milligan, B. J., Curtin, N. A. and Bone, Q. (1997). Contractile properties of obliquely striated muscle from the mantle of squid (*Alloteuthis subulata*) and cuttlefish (*Sepia officinalis*). *J. Exp. Biol.* **200**, 2425-2436.
Millman, B. M. (1967). Mechanism of contraction in Molluscan muscle. *Amer. Zool.* **7**, 583-591.
Moltschaniwskj, N. A. (1994). Muscle tissue growth and muscle fibre dynamics in the tropical loliginid squid *Photololigo sp.* (Cephalopoda: Loliginidae). *Can. J. Fish. Aquat. Sci.* **51**, 830-835.
Moltschaniwskj, N. A. (1995). Changes in shape associated with growth in the tropical loliginid squid *Photololigo sp.* : a morphometric approach. *Can. J. Zool.* **73**, 1335-1343.
Moltschaniwskj, N. A. (1997). Changes in mantle structure associated with growth and reproduction in the tropical loliginid squid *Photololigo sp.* (Cephalopoda: Loliginidae). *J. Moll. Stud.* **63**, 290-293.
Mommsen, T. P., Ballantyne, J., MacDonald, D., Gosline, J. and Hochachka, P. W. (1981). Analogues of red and white muscle in squid mantle. *Proc. Natl. Acad. Sci. USA* **78**, 3274-3278.

Moon, T. W. and Hulbert, W. C. (1975). The ultrastructure of the mantle musculature of the squid *Symplectoteuthis oualaniensis*. *Comp. Biochem. Physiol.* **52B**, 145-149.
Nichols, J. T., Moslemi, A. A. and Krueger, P. S. (2008). Performance of a self-propelled pulsed-jet vehicle. AIAA paper no. 2008-3720.
O'Dor, R. K. and Shadwick, R. E. (1989). Squid, the olympian cephalopods. *J. Ceph. Biol.* **1**, 33-55.
Perreault-Micale, C. L., Kalabokis, V. N., Nyitray, L. and Szent-Gyorgyi, A. G. (1996). Sequence variations in the surface loop near the nucleotide binding site modulate the ATP turnover rates of molluscan myosins. *J. Muscle Cell. Motil.* **17**, 543-553.
Preuss, T., Lebaric, Z. N. and Gilly, W. F. (1997). Post-hatching development of circular mantle muscles in the squid *Loligo opalescens*. *Biol. Bull.* **192**, 375-387.
Roberts, T. J., Marsh, R. L., Weyand, P. G. and Taylor, C. R. (1997). Muscular force in running turkeys: the economy of minimizing work. *Science* **275**, 1113-1115.
Rome, L. C., Syme, D. A., Hollingworth, S. L. and Lindstedt, S. M. (1996). The whistle and the rattle: the design of sound producing muscles. *Proc. Natl. Acad. Sci. USA* **93**, 8095-8100.
Rosenbluth, J. (1965). Ultrastructural organization of obliquely striated muscle fibers in *Ascaris lumbricoides*. *J. Cell Biol.* **25**, 495-515.
Rosenbluth, J. (1968). Obliquely striated muscle. IV. Sarcoplasmic reticulum, contractile apparatus, and endomysium of the body muscle of a polychaete, *Glycera,* in relation to its speed. *J. Cell Biol.* **36**, 245-259.
Schaeffer, P. J., Conley, K. E. and Lindstedt, S. L. (1996). Structural correlates of speed and endurance in skeletal muscle: The rattlesnake tailshaker muscle. *J. Exp. Biol.* **199**, 351-358.
Schiaffino, S. and Reggiani, C. (1996). Molecular diversity of myofibrillar proteins: gene regulation and functional significance. *Physiol. Rev.* **76**, 371-423.
Staron, R. S. and Pette, D. (1987). The multiplicity of combinations of myosin light-chains and heavy-chains in histochemically typed single fibers – rabbit soleus muscle. *Biochem. J.* **243**, 687-693.
Sweeney, H. L., Kushmerick, M. J., Mabuchi, K., Sréter, F. A. and Gergely, J. (1988). Myosin alkali light chain and heavy chain variations correlate with altered shortening velocity of isolated skeletal muscle fibers. *J. Biol. Chem.* **263**, 9034-9039.
Thompson, J. T. and Kier, W. M. (2001a). Ontogenetic changes in mantle kinematics during escape-jet locomotion in the oval squid, *Sepioteuthis lessoniana* Lesson, 1830. *Biol. Bull.* **201**, 154-166.
Thompson, J. T. and Kier, W. M. (2001b). Ontogenetic changes in fibrous connective tissue organization in the oval squid *Sepioteuthis lessoniana* Lesson, 1830. *Biol. Bull.* **201**, 136-153.
Thompson, J. T. and Kier, W. M. (2006). Ontogeny of circular muscle ultrastructure and implications for jet locomotion in Oval Squid, *Sepioteuthis lessoniana*. *J. Exp. Biol.* **209**, 433-443.
Thompson, J. T., Szczepanski, J. A. and Brody, J. (2008). Mechanical specialization of the obliquely striated circular mantle muscle fibres of the long-finned squid *Doryteuthis pealeii*. *J. Exp. Biol.* **211**, 1463-1474.
Toniolo, L., Maccatrozzo, L., Patruno, M., Pavan, E., Caliaro, F., Rossi, R., Rinaldi, C., Canepari, M., Reggiani, C. and Mascarello, F. (2007). Fiber types in canine muscles: myosin isoform expression and functional characterization. *Am. J. Physiol.* **292**, C1915-C1926.
Tu, M. S. and Dickinson, M. H. (1994). Modulation of negative work output from a steering muscle of the blowfly *Calliphora vicina*. *J. Exp. Biol.* **192**, 207-224.
Twarog, B. (1967). Factors influencing contraction and catch in *Mytilus* smooth muscle. *J. Physiol.* **192**, 847-856.
Venable, J. H. and Coggeshall, R. (1965). A simplified lead citrate stain for use in electron microscopy. *J. Cell Biol.* **25**, 407-408.
Ward, D. V. and Wainwright, S. A. (1972). Locomotory aspects of squid mantle structure. *J. Zool. Lond.* **167**, 437-449.
Williams, L. W. (1909). *The Anatomy of the Common Squid* Loligo pealii, *Lesueur*. New York: Leiden-Holland.
Woods, W. A., Fusillo, S. J. and Trimmer, B. A. (2008). Dynamic properties of a locomotory muscle of the tobacco hornworm *Manduca sexta* during strain cycling and simulated natural crawling. *J. Exp. Biol.* **211**, 873-882.
Young, J. Z. (1938). The functioning of the giant nerve fibres of the squid. *J. Exp. Biol.* **15**, 170-185.
Zeidberg, L. D. and Hamner, W. M. (2002). Distribution of squid paralarvae, *Loligo opalescens* (Cephalopoda: Myopsida), in the Southern California Bight in the three years following the 1997-1998 *El Niño*. *Mar. Biol.* **141**, 111-122.